

Low-temperature homoepitaxial growth of Pt(111) in simulated vapor deposition

Marie Villarba and Hannes Jónsson

Department of Chemistry, BG-10, University of Washington, Seattle, Washington 98195

(Received 2 August 1993)

Several atomic processes enhancing layer-by-layer growth have been identified in simulated deposition of Pt atoms onto Pt(111) at 275 K. After depositing the equivalent of one and two monolayers, only ca. 10% of the atoms sit atop the primary growing layer. Impinging atoms accelerate strongly towards the surface and can displace peripheral island atoms. Excess kinetic energy is generated that can effect annealing, even several atoms away from the impact site. Adatoms can descend at island edges only by an exchange diffusion mechanism, particularly at kink sites and vacancy islands.

Several experiments have indicated layer-by-layer growth of metals at remarkably low temperature. Egelhoff and Jacob observed reflection high-energy electron diffraction oscillations at 77 K in deposition of Cu on Cu(100).¹ Flynn, Evans, and Thiel made similar observations in deposition of Pd on Pd(100) at 80 K.² Poelsema and co-workers applied He atom scattering to the study of Pt(111) growth and observed surprisingly pronounced oscillations in the specular intensity near room temperature (275 K) and below.^{3,4} Since the diffuse He atom scattering cross section of surface defects is very large,⁵ the specular reflectivity is a clear sign of high degree of ordering at these low temperatures. A rapid and monotonic decay of the reflectivity was indeed observed at slightly *higher* temperatures (424 K), indicating that some ordering mechanisms are less effective at the higher temperatures. At still higher temperatures (621 K) clear layer-by-layer growth is observed. This kind of temperature dependence has been termed "reentrant" layer-by-layer growth and has subsequently been observed in several other systems.

Several theoretical and computer simulation studies of atom collisions with surfaces have been carried out. The thermal accommodation has been analyzed in simple models and found to be very fast due to multiphonon excitations.^{6,7} Computer simulations of metal atom collisions with surfaces have shown that the incident atoms get incorporated into the lattice at the site of impact, or at most one to two sites away.⁸ Evans *et al.* have emphasized that pyramidal structures on the surface can funnel atoms down to their base and this would lead to a narrower distribution of growing layers.⁹ However, pyramidal structures have negligible specular reflectivity for He atoms, so this effect is not sufficient to explain the high degree of reflectivity from the Pt(111) surfaces in the experiments of Poelsema *et al.*⁴

We have simulated the sequential deposition of Pt atoms onto Pt(111) substrate to mimic vapor deposition. The temperature of the substrate was kept at 275 K and the incoming kinetic energy of the vapor atoms 0.3 eV, typical for vapor at the melting temperature. The substrate consisted of layers with 90 atoms subject to periodic boundary conditions parallel to the surface. The classical dynamics were calculated using the velocity Verlet algorithm¹⁰ and analytically derived forces. A time step of

5 fsec was used, leading to fluctuations in the energy on the order of 1 part in 10^6 of the total energy. New vapor atoms are introduced into the system at regular intervals, ranging from 10 to 200 ps depending on the deposition rate. Just before the introduction of a new atom, all velocity components in the system are reassigned according to a Boltzmann distribution for the substrate temperature (massive collision) so as to remove the heat of condensation and to mimic the long equilibration time present in the laboratory measurements. The Pt interaction potential is of embedded-atom method type,¹¹

$$E_{\text{tot}} = \sum_{ij, i \neq j} \phi(r_{ij}) + \sum_i F(\rho_i),$$

where F_i and ρ_i are the embedding energy and electron density for atom i , and $\phi(r_{ij})$ is the pair interaction between atoms i and j separated by a distance r_{ij} . The potential was fitted to various bulk and dimer properties,¹² with $\phi(r_{ij})$ taken to be a Morse potential $\phi(r) = D(1 - e^{-\alpha(r-R)})^2 - D$ with depth D of 2.19 eV, a decay length of α of 1.83 \AA^{-1} , and reference position R of 2.35 Å. The density ρ_i is obtained by summing over "atomic electron densities" $\rho_i = \sum_{j \neq i} \rho^A(r_{ij})$ with $\rho^A(r) = r^6(e^{-3.64 \text{ \AA}^{-1}r} + 512e^{-7.28 \text{ \AA}^{-1}r})$. Both ϕ and ρ are cut and shifted at 5.5 Å to make the interaction range finite. The potential correctly predicts an energetic preference for the missing-row reconstruction of the Pt(110) face, and calculated surface relaxations are in good agreement with experiment, as has previously been found for similar potentials.¹³

As the vapor atoms approach the surface, they fall into a 4-eV potential well due to the binding to the surface. By the time they collide with the repulsive potential wall of the substrate, the kinetic energy of the impinging atoms is large, much larger than that of gas-phase vapor atoms. Figure 1 shows the time evolution of the excess energy at the site of impact. The average kinetic energy of the incident atom and six underlying atoms (in two layers) was calculated over intervals of 0.25 psec and is reported in units of temperature. The excess energy is removed in 2–3 psec (an adatom vibrational period is ca. 0.1 psec). For all deposition rates used in our simulations, the time between deposition events is much longer than this thermal accommodation time. Figure 1 also shows comparison between simulations at constant ener-

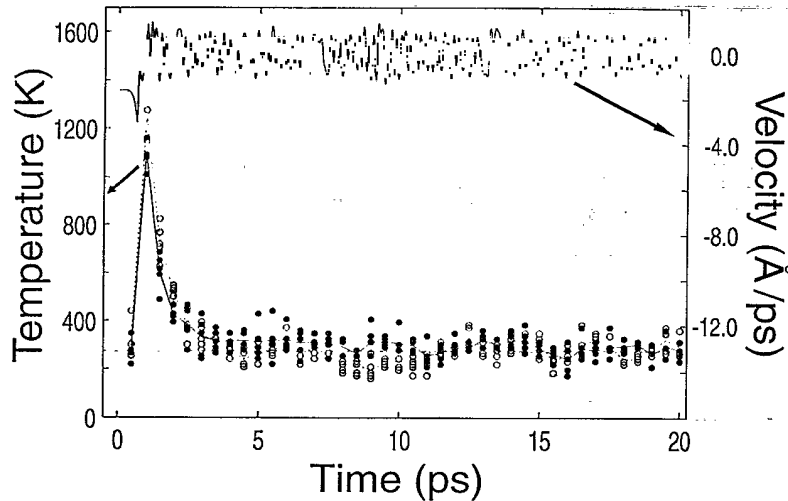


FIG. 1. Kinetic energy (in temperature units) averaged over 0.25 psec in a rectangular box containing the deposited atom and six atoms in the two layers directly below. The excess energy is removed very quickly, in ca. 2 psec. The filled circles are for five different impact parameters on the 14-layer substrate. The open circles are for a reduced 6-layer system including stochastic collisions in third and fourth layers. Upper curve shows how the excess velocity of the impinging atom (scale to the right) is lost in the first collision with the substrate.

gy with 14-layer substrate (the system is large enough that overall heating of the system due to condensation of one atom is only 15 degrees) and simulations with 6 layers where temperature is controlled in the third and fourth layer (lowest two layers are held rigid in both cases). The top curve in Fig. 1 shows how rapidly the incoming atom loses its kinetic energy. After the first collision with the surface atoms there is no sign of excess energy in the adatom.

Several deposition runs were carried out at various deposition rates. After depositing the equivalent of one monolayer (90 atoms), the fraction of atoms placed in the first growing layer was calculated, and is reported in Fig. 2 as the incorporation ratio. The rest of the deposited atoms sit in a second layer and, occasionally, third-layer sites. Longer time per deposition leads to higher incorporation rates on average [Fig. 2(a)]. A strong correlation exists between the incorporation ratio and the number of deposition events before trimer forms atop, as shown in Fig. 2(b). Isolated adatoms are quite mobile on the (111) surface (the calculated diffusion barrier is only 0.08 eV), while substantial barriers exist for descent of atoms from atop islands (see below). Dimers are also mobile in the simulation and have been observed to descend from atop an island. However, the diffusion of a trimer would require concerted motion of all three atoms so as not to break a nearest-neighbor bond. This does not occur on the time scale of the simulations. The trimers become nuclei for island growth in a new layer.

Figure 3 shows three kinds of events that enhance layer-by-layer growth and a final configuration after the equivalent of one monolayer has been deposited at the slowest deposition rate, 200 psec per deposition. Figure 3(a) shows an event where the incident atom impinges on a stable site atop an island but, without reversal of the perpendicular momentum of the incident atom, one of the underlying island atoms gets displaced by the incoming atom (as indicated by arrows in the figure). This type of event can only occur near island edges in Pt vapor deposition, so the probability is greatly enhanced when islands are small, irregular (incorporating vacancy islands), and have branched structure. Such displacements are therefore expected to be more important at lower

temperatures where edge diffusion is ineffective and islands are small and irregular. Similar events have been observed in other simulations of metal-vapor deposition.^{14,15} Since mechanism will be less effective at higher

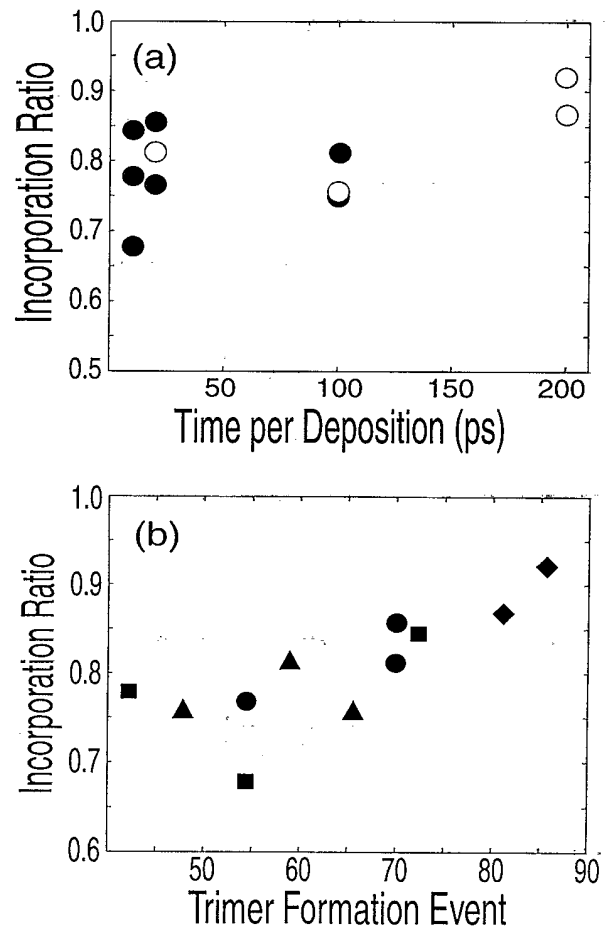


FIG. 2. The fraction of deposited atoms incorporated into the first layer is shown as a function of (a) the time per deposition (inverse deposition rate), (b) time before a trimer is formed atop the first layer, after deposition of the equivalent of one monolayer (90 atoms) at various deposition rates (filled circles for 14-layer substrate, open circles for reduced system).

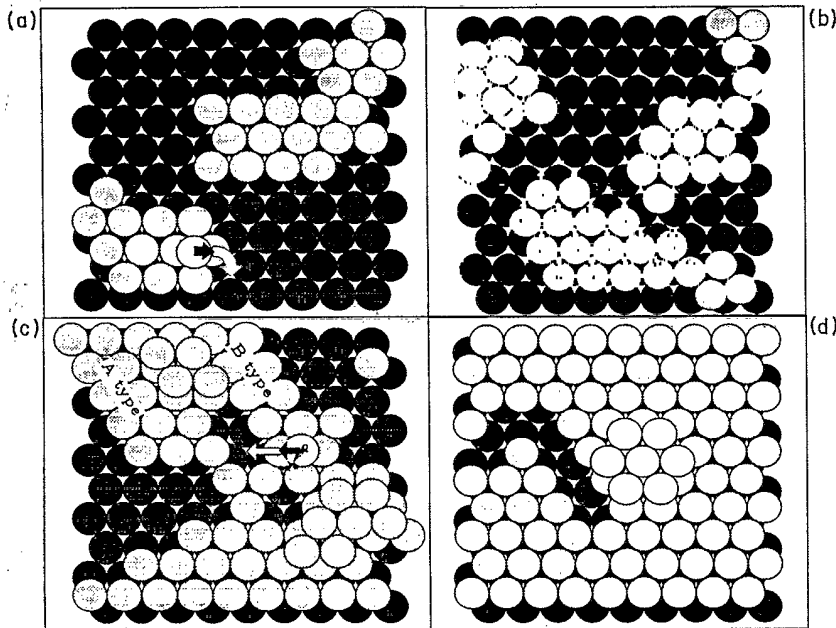


FIG. 3. Surface structure at various stages of deposition: (a)–(c) after 28, 46, and 72 atoms have been deposited in a 20-psec per deposition run, and (d) after the equivalent of one monolayer had been deposited in a 200-psec per deposition run. Various layer smoothing processes observed: (a) Displacement event; the deposited atom displaces a peripheral island atom as it impinges on an island. (b) Relaxation event; the deposition of an atom (open circle) induces annihilation of a grain boundary. (c) Exchange descent; the second layer atom initially occupies a near-fourfold-coordinated site (open circle). During the diffusion event, one of the underlying atoms moves out (open arrow) and the second-layer atom takes its place (filled arrow). Exchange descent was also observed at *B*-type edges, but never at straight *A*-type edges. (d) Final configuration after deposition of the equivalent of one monolayer.

temperature, it will likely contribute to the reentrant layer-by-layer growth. However, it is not likely to be the dominant effect because the islands are already much too large for displacement to be important in the temperature range where clear He atom oscillations are observed.¹⁶

Relaxation of previously deposited atoms due to the changing environment is an important contributor to the evolution of the surface morphology. An example is shown in Fig. 3(b), where the addition of an atom in between two islands of different grain results in coalescence of the islands and therefore elimination of what would have developed into a grain boundary. There is no activation barrier for this event. Furthermore, an area of excess energy created at the surface by an impinging atom can fuel thermally activated processes involving nearby atoms. We have observed diffusion events, such as descent from atop islands, which coincide clearly with a nearby impact by a vapor atom.

The descent of atoms from atop islands by a simple hop over the island edge has a large energy barrier of 0.70–0.85 eV depending on the geometry, and is never observed in the simulations. However, atoms are observed to descend via a two-atom exchange process as illustrated in Fig. 3(c). Such an exchange process has been observed by field ion microscopy of Ir(111).¹⁷ We have evaluated the energy barriers for the various diffusion processes us-

ing a method where several (typically 30) replicas of the system are connected with elastic restoring force and relaxed to a minimum energy configuration.

There are two types of steps on the (111) surface, *A* type and *B* type, with quite different energy barriers for exchange descent. The straight *A*-type step has a higher barrier, 0.32 eV, while the barrier is 0.18 eV at the *B*-type step. Furthermore, a kink site at the *B*-type step does not offer a lower-energy path for descent, while a kink on the *A*-type step opens a path with barrier as low as 0.11 eV. This qualitative difference can be relevant to the fact that triangular islands with nearly straight *A*-type edges are observed in scanning tunneling microscopy (STM) images at 400 K.¹⁹ Adatoms will preferably descend at *B*-type edges leading to faster advancement of that step edge, while the straight *A*-type edge survives during the growth process. An adatom arriving at the rough *B*-type edge will be trapped easily by a nearby kink. When islands surrounded by only *A*-type edges have formed, the tendency for three-dimensional growth will be much greater, because of the larger energy barrier for adatoms to descend from atop the islands. Monotonic decay of

TABLE I. Fate of atoms deposited on top of islands in the growing layer during deposition of the first monolayer (90 atoms). An average was taken over two runs for each deposition rate.

| | 100 psec per deposition | 200 psec per deposition |
|--------------------|-------------------------|-------------------------|
| Displacement | 19% | 18% |
| Exchange diffusion | 28% | 57% |
| Remaining atop | 53% | 25% |

TABLE II. Breakdown of the exchange diffusion events observed during runs with 200 psec per deposition event. The events are classified according to the final coordination of the displaced atom within the surface plane. Coordination of 2 means the event occurred at a straight edge site, coordination 3 corresponds to a kink site, etc.

| Coordination no. of displaced atom | Fraction of the observed exchange events |
|------------------------------------|--|
| 2 | 6% |
| 3 | 38% |
| 4 | 28% |
| 5 | 19% |
| 6 | 9% |

the He atom reflectivity is indeed observed³ in the temperature range where STM images show islands with mostly A-type step edges.²⁰

Table I gives results from detailed analysis of four deposition simulations. It shows that, on average, atoms impinging on top of islands have 10–15 % probability of making it into the growing layer via a displacement mechanism. A larger fraction of the atoms descend by an exchange event after partial or full thermal accommodation with the substrate. The probability for such an event is larger in the longer simulation runs, since adatoms are mobile on the time scale of the simulation. Table II gives the breakdown of the exchange events according to the local environment, which is well characterized by the final coordination of the displaced atom in the surface plane. Most of the exchanges occur at kink sites (coordination number 3) and at vacancy islands which form as islands start to coalesce. Figure 4 shows the filling of the first and subsequent layers as the deposition is continued. While the first layer was filled to a large extent before the second layer started growing appreciably, by the time three monolayers (270 atoms) have been deposited the surface is growing on four different levels. This would result in rapid decay of interference oscillations in a reflected He atom beam. Simulations with larger samples and evaluation of the He atom reflectivity is in progress.

We gratefully acknowledge helpful discussions with Professor Bene Poelsema and Dr. T. Michely. We thank

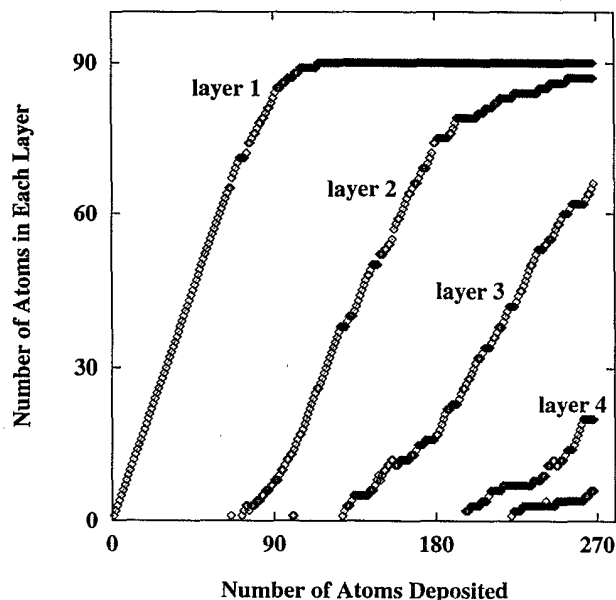


FIG. 4. Layer filling during deposition of three monolayers. The first layer is nearly full by the time the second layer starts filling in appreciably. At the end, four different layers are growing simultaneously.

Alex Goldstein for help in developing and implementing the interaction potential. This work has been supported by NSF under Grant No. CHE-61-2365, by ACS-PRF and DOE-BES.

- ¹W. F. Egelhoff, Jr. and I. Jacob, *Phys. Rev. Lett.* **62**, 921 (1989).
- ²D. K. Flynn, J. W. Evans, and P. A. Thiel, *J. Vac. Sci. Technol. A* **7**, 2162 (1989).
- ³R. Kunkel, B. Poelsema, L. K. Verheij, and G. Comsa, *Phys. Rev. Lett.* **65**, 733 (1990).
- ⁴B. Poelsema, R. Kunkel, N. Nagel, A. F. Becker, G. Rosenfeld, L. K. Verheij, and G. Comsa, *Appl. Phys. A* **53**, 369 (1991).
- ⁵B. Poelsema and G. Comsa, *Scattering of Thermal Energy Atoms from Disordered Surfaces* (Springer, Berlin, 1989).
- ⁶R. W. Zwanzig, *J. Chem. Phys.* **32**, 1173 (1960).
- ⁷F. O. Goodman, *J. Phys. Chem. Solids* **23**, 1491 (1962).
- ⁸D. E. Sanders and A. E. DePristo, *Surf. Sci.* **254**, 341 (1991).
- ⁹J. W. Evans, D. E. Sanders, P. A. Thiel, and A. E. DePristo, *Phys. Rev. B* **41**, 5410 (1990).

- ¹⁰H. C. Andersen, *J. Chem. Phys.* **72**, 2384 (1980).
- ¹¹A. F. Voter and S. P. Chen, in *Characterization of Defects in Materials*, edited by R. W. Siegel, J. R. Weertman, and R. Sinclair, MRS Symposia Proceedings No. 82 (Materials Research Society, Pittsburgh, 1987), p. 175.
- ¹²A. Goldstein and H. Jónsson (unpublished).
- ¹³M. S. Daw, *Phys. Rev. B* **39**, 7441 (1989).
- ¹⁴P. Stoltze and J. K. Norskov (unpublished).
- ¹⁵R. Wang and K. A. Fichthorn (unpublished).
- ¹⁶B. Poelsema (private communication).
- ¹⁷S. C. Wang and G. Ehrlich, *Phys. Rev. Lett.* **67**, 2509 (1991).
- ¹⁸H. Jónsson and G. Mills (unpublished).
- ¹⁹T. Michely, M. Hohage, M. Bott, and G. Comsa, *Phys. Rev. Lett.* **70**, 3943 (1993).